Gravitational wave probes of axionlike particles

Camila S. Machado,* Wolfram Ratzinger,† Pedro Schwaller,‡ and Ben A. Stefanek§

PRISMA Cluster of Excellence and Mainz Institute for Theoretical Physics, Johannes Gutenberg-Universität Mainz, 55099 Mainz, Germany

(Received 18 March 2020; accepted 29 September 2020; published 27 October 2020)

We have recently shown that axions and axionlike particles (ALPs) may emit an observable stochastic gravitational wave (GW) background when they begin to oscillate in the early Universe. In this note, we identify the regions of ALP parameter space, which may be probed by future GW detectors, including ground- and space-based interferometers, and pulsar timing arrays. Interestingly, these experiments have the ability to probe axions from the bottom up, i.e., in the very weakly coupled regime, which is otherwise unconstrained. Furthermore, we discuss the effects of finite dark photon mass and kinetic mixing on the mechanism, as well as the (in)sensitivity to couplings of the axion to Standard Model fields. We conclude that realistic axion and ALP scenarios may indeed be probed by GW experiments in the future and provide signal templates for further studies.

DOI: 10.1103/PhysRevD.102.075033

I. INTRODUCTION

The direct detection of gravitational waves (GW) opened up a new avenue to explore fundamental physics in the early Universe. In particular, axions or axionlike particles (ALPs) are a well-motivated extension of the Standard Model (SM), e.g., to solve the strong *CP* problem [1], to provide a dynamical solution to the electroweak hierarchy problem [2], to provide suitable inflaton [3] or dark matter (DM) candidates [4–6], or in the context of string theory [7]. Experimental searches for these particles are covering an increasing part of the parameter space. Several searches rely on the axion-photon coupling, which is generically inversely proportional to the axion decay constant. This means the region corresponding to smaller decay constants (larger couplings) is more constrained, whereas larger values are usually difficult to probe.

In Ref. [8], we showed that axions or axionlike particles coupled to a light dark photon can produce a stochastic gravitational wave background (SGWB) when the axion field begins to oscillate in the early Universe, allowing exploration of parameter space inaccessible to experiments that rely on the axion-photon coupling. The rolling axion induces a tachyonic instability that amplifies vacuum fluctuations of a single gauge boson helicity, sourcing chiral GWs. The energy transfer from the axion into light vectors also widens the viable parameter space for axion DM.

The goal of this paper is to explore the phenomenological impact of our findings. First, we show that GWs can be produced in realistic axion and ALP scenarios, where other couplings such as kinetic mixing of the SM and dark photon, couplings of the axion to SM fields, or nonzero dark photon masses are also present. Next, we provide a simple analytic fit to the GW spectrum extracted from our numerical simulation, useful for further studies or comparison with GW signals from other sources. We present the main result of our paper in Fig. 2, where we identify the regions of ALP parameter space that will be probed by future GW experiments. Since a strong polarization of the GW signal peak is a firm prediction of our scenario, in Fig. 3, we indicate the region where this feature may be probed following the recent results of Ref. [9]. It is striking that gravitational waves may be able to provide evidence for axions with very large decay constants, which are otherwise inaccessible.

II. THE AUDIBLE AXION MODEL

Here, we give a brief overview of the model presented in Ref. [8], which consisted of an axion field ϕ and a massless dark photon X_μ of an unbroken $U(1)_X$ Abelian gauge group,

$$\frac{\mathcal{L}}{\sqrt{-g}} = \frac{1}{2}\partial_\mu\phi\partial^\mu\phi - V(\phi) - \frac{1}{4}X_{\mu\nu}X^{\mu\nu} - \frac{\alpha}{4f}\phi X_{\mu\nu}\tilde{X}^{\mu\nu}, \quad (1)$$

*camachad@uni-mainz.de
†w.ratzinger@uni-mainz.de
‡pedro.schwaller@uni-mainz.de
§bstefan@uni-mainz.de

where the parameter f is the scale at which the global symmetry corresponding to the Nambu-Goldstone field ϕ is broken [10]. We assume this global symmetry is also explicitly broken at the scale $\Lambda \sim \sqrt{mf}$, resulting in the potential $V(\phi)$ and a mass m for the axion.

While the expansion rate of the Universe $H = a'/a^2$ is greater than the axion mass m, the axion field is overdamped and does not roll [11]. In a radiation-dominated Universe, H becomes of order m at the temperature $T_{\rm osc} \approx \sqrt{mM_P}$, at which point, the axion will begin to oscillate in its potential with initial conditions given by misalignment arguments, namely, $\phi_i = \theta f$, $\phi'_i \approx 0$, and $\theta \sim \mathcal{O}(1)$, where θ is the initial misalignment angle. The $\phi X_{\mu\nu}\tilde{X}^{\mu\nu}$ coupling results in a nontrivial dispersion relation for the gauge field helicities,

$$\omega_\pm^2(k,\tau) = k^2 \mp k\frac{\alpha}{f}\phi', \tag{2}$$

that depends explicitly on the velocity ϕ' of the axion field. As the axion field oscillates, one of the gauge field helicities will have a range of modes with imaginary frequencies (negative ω^2), resulting in a tachyonic instability that drives exponential growth. This process transfers energy from the axion field into dark gauge bosons and amplifies vacuum fluctuations of the tachyonic modes into a rapidly time-varying, anisotropic energy distribution that sources GWs. For an in-depth review of the particle production process and its applications, see Refs. [12–41]. We will now briefly discuss some possible extensions to the original simplified model.

A. Finite dark photon mass

First, we consider the possibility of a nonzero mass for the dark photon which could arise through a dark Higgs or Stueckelberg mechanism. The main effect of m_X is to modify the dark photon dispersion relation,

$$\omega_\pm^2(k,\tau) = k^2 + a^2 m_X^2 \mp k\frac{\alpha}{f}\phi', \tag{3}$$

which can reduce the efficiency of or prevent tachyonic growth. To further quantify this statement, we go back to the analysis in Ref. [8], where we showed that the tachyonic growth of the mode functions becomes inefficient if they grow less than $\mathcal{O}(1)$ during one oscillation of the axion field. This happens when $-\omega_\pm^2 < (am)^2$ is satisfied for all modes k. From this, we can deduce that for $\alpha\theta \gtrsim 10$, we require $m_X \lesssim \theta\alpha m/2$ in order to have tachyonic production. Here, we focus on dark photon masses well below this bound, which will not affect the success of our mechanism. The case where this is not true is discussed in the Supplemental Material [42].

B. Kinetic Mixing

Next, we examine whether the relevant photon-dark photon kinetic mixing operator,

$$\Delta\mathcal{L} = -\frac{\epsilon}{2}F_{\mu\nu}X^{\mu\nu}, \tag{4}$$

affects our mechanism. Indeed, this operator will inevitably be generated by renormalization group flow if there exist states, which carry both electromagnetic and $U(1)_X$ charge [43]. If kinetic mixing leads to an effective coupling of the dark photon to the SM radiation bath, one might worry that it induces a large thermal mass for the dark photon that prevents tachyonic growth.

In the case of an exactly massless dark photon $m_X = 0$, the kinetic mixing term is unphysical as it can be removed via the field redefinition $X' = X + \epsilon A$ and $A' = A/\sqrt{1-\epsilon^2}$ that leaves the coupling of the SM photon to the electromagnetic current unchanged. Thus, it is clear that only the field combination that couples to the SM plasma A' develops a thermal mass.

However, for $m_X \neq 0$, the mixing is physical. Diagonalizing the kinetic terms by performing the same field redefinition now leads to a nondiagonal mass matrix which, in addition to the thermal mass Π induced by the SM plasma for A', must be included in the dispersion relation,

$$\left[\omega^2 + k^2 + \begin{pmatrix} \epsilon'^2 m_X^2 + \Pi & -\epsilon' m_X^2 \\ -\epsilon' m_X^2 & m_X^2 \end{pmatrix}\right]\begin{pmatrix} A'^\mu \\ X'^\mu \end{pmatrix} = 0, \tag{5}$$

with $\epsilon' = \epsilon/\sqrt{1-\epsilon^2}$. The photon thermal mass is of order $\Pi \approx e^2T^2$, which at the time when the axion begins to oscillate evaluates to $\Pi \approx e^2 m M_P$. As discussed in Sec. II A, the existence of the tachyonic instability requires $m_X \lesssim \theta\alpha m/2$. Furthermore, the momenta that experience tachyonic growth are those with $k \lesssim \theta\alpha m$, so we are deeply in the regime, where $m_X^2, k^2 \ll \Pi$. In this limit, the effective mass matrix in Eq. (5) always has a small eigenvalue $m_X^2(1 + \mathcal{O}(\epsilon^2))$, which is independent of T^2, despite the kinetic mixing [44,45]. Thus, we conclude that the field combination associated with the dark photon X' does not acquire a thermal mass via kinetic mixing, so we are subject only to the usual constraints on ϵ, see, e.g., Refs. [46–59].

C. QCD axion

Finally, we examine the case, where the ALP ϕ is taken to be the QCD axion itself, which is the focus of Ref. [29]. In this limit, m and f are not independent parameters but are instead related by $m^2 f^2 = \chi_{\rm QCD}$, where $\chi_{\rm QCD} = (75.5\ \mathrm{MeV})^4$ is the QCD topological susceptibility. In particular, the QCD axion has the following couplings to SM gauge bosons:

$$\Delta\mathcal{L} = \frac{\alpha_s}{8\pi f}\phi G^a_{\mu\nu}\tilde{G}^{a\,\mu\nu} + \frac{g_{\phi\gamma\gamma}}{4}\phi F^{\mu\nu}\tilde{F}_{\mu\nu}, \quad (6)$$

where $G^a_{\mu\nu}$ and $F_{\mu\nu}$ are the gluon and photon field strengths, respectively, and $g_{\phi\gamma\gamma}$ is a model dependent coupling, e.g., $g_{\phi\gamma\gamma} = -1.92\alpha_{\rm EM}/(2\pi f)$ in the KSVZ model [60,61]. Here, we note that none of these couplings spoil the effectiveness of our mechanism because the tachyonic growth of these states are regulated by plasma effects. The photon acquires a Debye mass of order $\Pi \sim e^2T^2$ via hard thermal loops, preventing tachyonic growth [62,63]. Similarly, the gluon self-coupling induces a magnetic mass, $m(T) \sim g^2T$ [64–66]. As a final consideration, model dependent couplings of ϕ to SM fermions also exist. However, the production of fermions is not exponential due to Pauli blocking. Thus, the exponential production of dark photons dominates over SM channels.

III. GRAVITATIONAL WAVE SPECTRUM

Here, we present an improved computation of the GW spectrum as compared to the results of Ref. [8]. The computation requires the discretization of a double integral over the tachyonic momenta, resulting in the simulation time growing as the square of the number of gauge modes. By switching to a more memory efficient code written in Python, we were able to solve the coupled axion-gauge boson equations of motion using $N = 10^5$ gauge modes. For the GW spectrum computation, an $N_{\rm GW} = 500$ subset of these modes were taken, which is an order of magnitude improvement over our previous simulation. We show the results of the improved numerical calculation in Fig. 1. The spectrum is strongly polarized in the peak region, whereas the tail is unpolarized as shown in the figure. Note that backscattering effects (not included here) could affect the degree of polarization at high frequencies [39]. Furthermore, the dashed green line indicates a

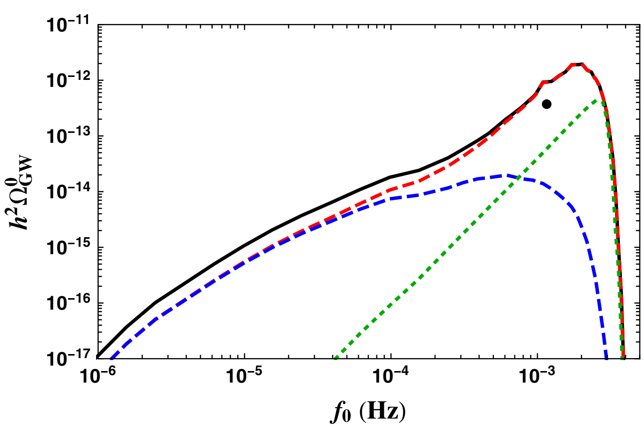

FIG. 1. GW spectra from the improved numerical simulation for the ALP2 benchmark point of Ref. [8]. Black is the total spectrum, whereas red and blue are the individual polarizations. Green gives the "conservative spectrum" as described in Sec. III.

"conservative spectrum," which is the part we expect to remain even if the process of gauge bosons backscattering into axions results in a strong backreaction [67]. In any case, we expect the GWs produced during the initial tachyonic instability phase to survive, and we use the estimate for the closure of the tachyonic band given in Ref. [8] to obtain the conservative spectrum shown in Fig. 1.

A. GW spectrum fit template

To make connection with experimental searches for SGWBs, we use the improved numerical simulation to extract a GW signal template. Such a template enables simple estimates of the GW spectrum and signal-to-noise (SNR) calculations for a given set of model parameters, without having to run a complicated numerical simulation. We approach our GW signal template from the ansatz that the low frequency part of the GW spectrum is given by a power law while the high frequency part falls off exponentially, with some transition region that gives the peak. A reasonable ansatz of this form is

$$\tilde{\Omega}_{\rm GW}(\tilde{f}) = \frac{\mathcal{A}_s(\tilde{f}/f_s)^p}{1+(\tilde{f}/f_s)^p\exp[\gamma(\tilde{f}/f_s-1)]}, \quad (7)$$

where $\tilde{\Omega}_{\rm GW} \equiv \Omega_{\rm GW}(f)/\Omega_{\rm GW}(f_{\rm peak})$ and $\tilde{f} \equiv f/f_{\rm peak}$. In Ref. [8], we derived simple analytic scaling relations for the peak amplitude and frequency of the GW spectrum, which at the time of GW emission are

$$f_{\rm peak} \approx (\alpha\theta)^{2/3}m, \qquad \Omega_{\rm GW}(f_{\rm peak}) \approx \left(\frac{f}{M_P}\right)^4\left(\frac{\theta^2}{\alpha}\right)^{\frac{4}{3}}, \quad (8)$$

where these expressions hold for $\alpha \sim 10$–100. The parameters $\mathcal{A}_s$ and f_s are fit to the GW spectrum from our numerical simulation to correct for the $\mathcal{O}(1)$ factors by which the scaling relation is off. The parameter p specifies the power law index and γ controls how quickly the exponential behavior takes over at high frequencies. Discussion of the fit to the simulation and the best fit values for the parameters A_s, f_s, γ, p can be found in the Supplemental Material [42]. Together, Eqs. (7) and (8) allow one to go directly from the underlying fundamental model parameters α, m, f to the GW spectrum.

IV. PROBING AUDIBLE AXION MODELS

With the results of the previous section, we can now identify the regions of parameter space that may be probed by future GW experiments. Detectability requires an SNR above a certain experiment dependent threshold. Here, we use the values and method of Ref. [68]. Our results are shown in Fig. 2, where the detectable regions lie below the curves labeled as SKA, LISA, BBO, DECIGO, and ET, respectively [69]. Interestingly, GW experiments are most

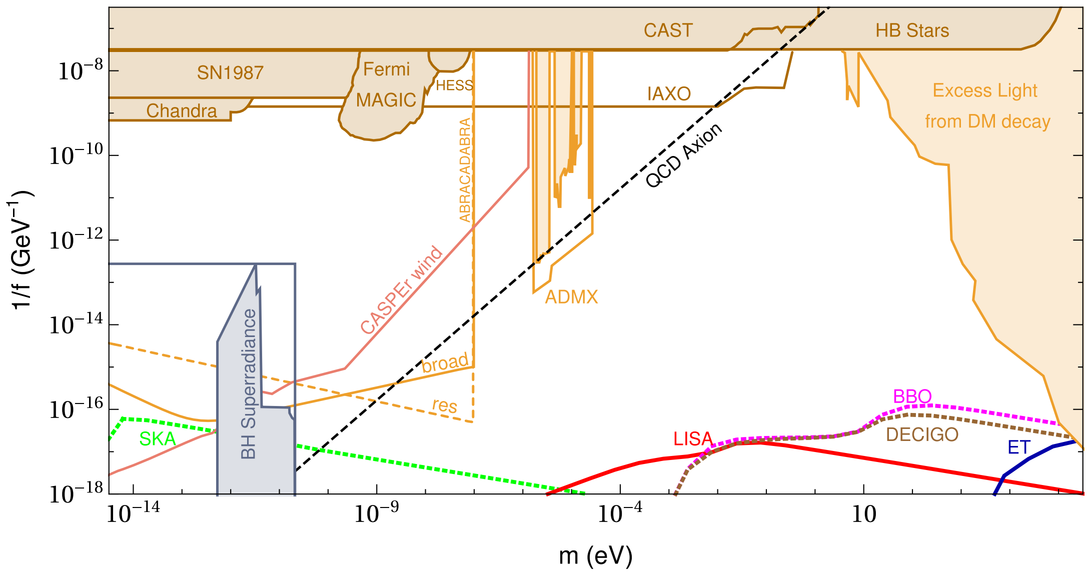

FIG. 2. Axion and ALP parameter space in the mass vs inverse decay constant plane. Regions below the colored curves are in reach of future ground-based (ET) and satellite-based (LISA, BBO, DECIGO) GW detectors, or future pulsar timing arrays (SKA). Shaded regions are excluded by existing constraints, while unshaded regions show the sensitivity of various other planned experiments. Black hole superradiance excludes the grey shaded region, and future black hole observations could extend this region to the grey line. The location of the QCD axion band is indicated by the black dashed line.

sensitive for large values of the decay constant f corresponding to very weakly coupled axions. These probes are therefore highly complementary to other existing limits (orange shaded) or planned searches (orange lines), which are typically more sensitive for larger couplings. An exception is the constraint coming from black hole superradiance (gray shaded), which is also most reliable for large decay constant f and also indirectly relies on GW observations [70,71]. It should also be emphasized that the GW signal regions do not depend on the axion relic abundance today and therefore, do not require the axion to account for all of DM. The nondecoupling behavior of the GW signal is due to the fact that larger f corresponds to more energy in the axion field $\Omega_\phi^{\mathrm{osc}} \propto m^2\theta^2 f^2$, which is available to be converted into gravitational radiation. This holds as long as the initial misalignment angle θ takes on natural values of $\mathcal{O}(1)$ [72]. Indeed, for our numerical results here, $\theta = 1$ is chosen.

In Fig. 3, we show a close up of the parameter space that leads to detectable signals, as well as bounds arising from cosmology. If the dark photon stays relativistic until recombination, the number of effective relativistic degrees of freedom N_{eff} sets an upper bound on the decay constant f. A simple estimate can be done assuming that all the energy in the axion field is converted into dark gauge bosons. This leads to a bound of $f \lesssim (5\text{–}7) \times 10^{17}$ GeV shown in Fig. 3, depending on whether the axion starts oscillating before or after the QCD phase transition. The dark photon might also become nonrelativistic before recombination and therefore, contribute to DM, as in Refs. [31–34]. The shaded green region of Fig. 3 shows the potential parameter space for vector DM (VDM), which is cut off at the lower bound of $f \approx 3 \times 10^{16}$ GeV, where the dark photons are too hot to be compatible with structure

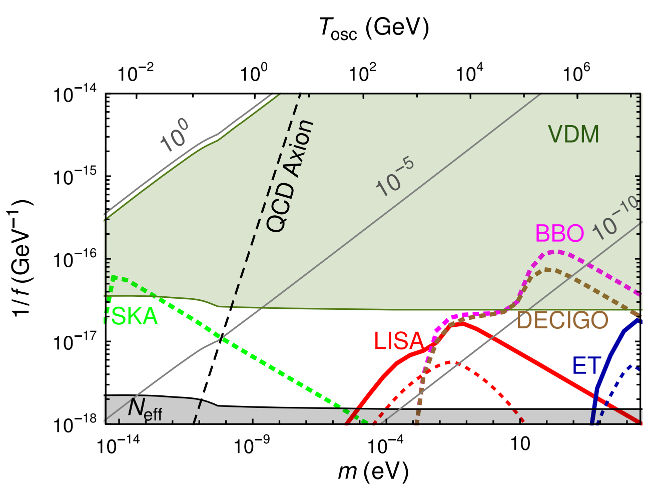

FIG. 3. Cosmological constraints on the model. The green shaded region indicates where dark photons could be vector dark matter (VDM), while the region labeled N_{eff} is excluded by constraints on the number of relativistic degrees of freedom. Furthermore, the required suppression of the axion abundance is indicated by the diagonal gray lines, in order not to overproduce axion DM. As before, the colored curves show the regions accessible to future GW experiments. In addition, we also show the region where LISA (dashed red) or ET (dashed blue) can detect the chirality of the GW signal.

formation. The Supplemental Material [42] contains additional information on the derivation of these bounds. The diagonal gray lines indicate how much the axion abundance must be suppressed compared to the ordinary misalignment case to avoid overproduction [73].

A smoking gun for audible axion models is the completely chiral nature of the peak of the GW spectrum, inherited from the parity violation in the dark photon population [8]. This can provide powerful background rejection, since SGWBs from astrophysical sources are not expected to carry a net polarization. It has been pointed out that the dipolar anisotropy induced by the Doppler shift due to the relative motion of our Solar System with respect to the cosmic reference frame can be exploited to allow planar detectors to detect net circular polarization [74–78]. In particular, LISA and ET would be able to detect net circular polarization with an SNR of $\mathcal{O}(1)$ for a SGWB with an amplitude $h^2\Omega_{\mathrm{GW}} \sim 10^{-11}$ [9]. In Fig. 3, we indicate using dashed lines in the region in parameter space, where the signal is strong enough such that LISA and ET can pick up on the polarization following the analysis of Ref. [9]. Of course, if a network of noncoplanar detectors is available in a particular frequency range, GW polarization can be detected without paying the $\mathcal{O}(10^{-3})$ suppression factor due to our peculiar velocity [74,79].

V. DISCUSSION AND CONCLUSIONS

In [8], we showed that a SGWB can be produced by an axion coupled to a dark photon, specifically by the tachyonic instability induced in the dark photon by the axion dynamics. This instability leads to an exponential growth of dark photon vacuum fluctuations which act as the GW source. Here, we have shown that this GW signal is also produced for a broader class of models that allow for a massive dark photon and/or kinetic mixing with the SM photon. Furthermore, we argue that couplings of the axion to gluons and photons do not affect the success of the mechanism, which illustrates the viability of the QCD axion case.

The central results of our paper are Figs. 2 and 3, where we show the regions of axion parameter space that may be probed by future GW experiments. Since the GW signal is strongest for large decay constants, GWs probe complementary regions of parameter space to most other experiments relying on couplings of the axion to the visible sector (proportional to the inverse of the decay constant) that are sizeable. In Fig. 3, we zoom in on the GW signal region and show cosmological constraints as well as the region where the dark photon itself could be DM. For most of the parameter space relevant for GW detectors, the axion relic abundance needs to be strongly suppressed, which might require an extension of the model.

Since the shape of the GW signal is universal for dark photon masses less than roughly the axion mass, we provide a fit template function which parametrizes the dependence of the GW amplitude and peak frequency on the axion mass m and decay constant f. This fit, which is extracted from our new simulation with an order of magnitude higher mode density, provides a quick translation from the underlying model parameters to the detectability of the GW signal for all experiments and parameter points, providing a tool which can be directly used by experimental collaborations to probe our and similar models.

ACKNOWLEDGMENTS

We would like to thank Masha Baryakhtar for illuminating discussions regarding the black hole superradiance constraints. The work of C. S. M. was supported by the Alexander von Humboldt Foundation, in the framework of the Sofja Kovalevskaja Award 2016, endowed by the German Federal Ministry of Education and Research. Work of W. R. was partially funded by the Deutsche Forschungsgemeinschaft (DFG), Project ID No. 438947057. We also acknowledge support by the Cluster of Excellence "Precision Physics, Fundamental Interactions, and Structure of Matter" (PRISMA$^+$ EXC 2118/1) funded by the German Research Foundation (DFG) within the German Excellence Strategy (Project ID No. 39083149).

[1] R. D. Peccei and H. R. Quinn, CP Conservation in the Presence of Pseudoparticles, Phys. Rev. Lett. **38**, 1440 (1977).
[2] P. W. Graham, D. E. Kaplan, and S. Rajendran, Cosmological Relaxation of the Electroweak Scale, Phys. Rev. Lett. **115**, 221801 (2015).
[3] K. Freese, J. A. Frieman, and A. V. Olinto, Natural Inflation with Pseudo Nambu-Goldstone Bosons, Phys. Rev. Lett. **65**, 3233 (1990).
[4] J. Preskill, M. B. Wise, and F. Wilczek, Cosmology of the invisible axion, Phys. Lett. **120B**, 127 (1983).
[5] L. F. Abbott and P. Sikivie, A cosmological bound on the invisible axion, Phys. Lett. **120B**, 133 (1983).
[6] M. Dine and W. Fischler, The not so harmless axion, Phys. Lett. **120B**, 137 (1983).
[7] A. Arvanitaki, S. Dimopoulos, S. Dubovsky, N. Kaloper, and J. March-Russell, String axiverse, Phys. Rev. D **81**, 123530 (2010).

[8] C. S. Machado, W. Ratzinger, P. Schwaller, and B. A. Stefanek, Audible axions, J. High Energy Phys. 01 (2019) 053.

[9] V. Domcke, J. Garcia-Bellido, M. Peloso, M. Pieroni, A. Ricciardone, L. Sorbo, and G. Tasinato, Measuring the net circular polarization of the stochastic gravitational wave background with interferometers, J. Cosmol. Astropart. Phys. 05 (2020) 028.

[10] We consider $\alpha > 1$ in order to have efficient particle production, which can be obtained in several UV completions, see e.g., [80].

[11] Here, primes denote derivatives with respect to conformal time.

[12] B. Ratra, Cosmological 'seed' magnetic field from inflation, Astrophys. J. **391**, L1 (1992).

[13] W. D. Garretson, G. B. Field, and S. M. Carroll, Primordial magnetic fields from pseudo-Goldstone bosons, Phys. Rev. D **46**, 5346 (1992).

[14] G. B. Field and S. M. Carroll, Cosmological magnetic fields from primordial helicity, Phys. Rev. D **62**, 103008 (2000).

[15] D.-S. Lee, W.-l. Lee, and K.-W. Ng, Primordial magnetic fields from dark energy, Phys. Lett. B **542**, 1 (2002).

[16] L. Campanelli and M. Giannotti, Magnetic helicity generation from the cosmic axion field, Phys. Rev. D **72**, 123001 (2005).

[17] M. M. Anber and L. Sorbo, N-flationary magnetic fields, J. Cosmol. Astropart. Phys. 10 (2006) 018.

[18] M. M. Anber and L. Sorbo, Naturally inflating on steep potentials through electromagnetic dissipation, Phys. Rev. D **81**, 043534 (2010).

[19] N. Barnaby and M. Peloso, Large Nongaussianity in Axion Inflation, Phys. Rev. Lett. **106**, 181301 (2011).

[20] N. Barnaby, R. Namba, and M. Peloso, Phenomenology of a pseudo-scalar inflaton: Naturally large nongaussianity, J. Cosmol. Astropart. Phys. 04 (2011) 009.

[21] N. Barnaby, E. Pajer, and M. Peloso, Gauge field production in axion inflation: Consequences for monodromy, non-gaussianity in the CMB, and gravitational waves at interferometers, Phys. Rev. D **85**, 023525 (2012).

[22] N. Barnaby, R. Namba, and M. Peloso, Observable non-gaussianity from gauge field production in slow roll inflation, and a challenging connection with magnetogenesis, Phys. Rev. D **85**, 123523 (2012).

[23] P. Adshead, E. Martinec, and M. Wyman, Gauge fields and inflation: Chiral gravitational waves, fluctuations, and the Lyth bound, Phys. Rev. D **88**, 021302 (2013).

[24] P. Adshead, J. T. Giblin, T. R. Scully, and E. I. Sfakianakis, Gauge-preheating and the end of axion inflation, J. Cosmol. Astropart. Phys. 12 (2015) 034.

[25] J. T. Giblin, G. Kane, E. Nesbit, S. Watson, and Y. Zhao, Was the universe actually radiation dominated prior to nucleosynthesis?, Phys. Rev. D **96**, 043525 (2017).

[26] A. Hook and G. Marques-Tavares, Relaxation from particle production, J. High Energy Phys. 12 (2016) 101.

[27] V. Domcke, M. Pieroni, and P. Binétruy, Primordial gravitational waves for universality classes of pseudoscalar inflation, J. Cosmol. Astropart. Phys. 06 (2016) 031.

[28] N. Kitajima, T. Sekiguchi, and F. Takahashi, Cosmological abundance of the QCD axion coupled to hidden photons, Phys. Lett. B **781**, 684 (2018).

[29] P. Agrawal, G. Marques-Tavares, and W. Xue, Opening up the QCD axion window, J. High Energy Phys. 03 (2018) 049.

[30] N. Fonseca, E. Morgante, and G. Servant, Higgs relaxation after inflation, J. High Energy Phys. 10 (2018) 020.

[31] J. A. Dror, K. Harigaya, and V. Narayan, Parametric resonance production of ultralight vector dark matter, Phys. Rev. D **99**, 035036 (2019).

[32] R. T. Co, A. Pierce, Z. Zhang, and Y. Zhao, Dark photon dark matter produced by axion oscillations, Phys. Rev. D **99**, 075002 (2019).

[33] M. Bastero-Gil, J. Santiago, L. Ubaldi, and R. Vega-Morales, Vector dark matter production at the end of inflation, J. Cosmol. Astropart. Phys. 04 (2019) 015.

[34] P. Agrawal, N. Kitajima, M. Reece, T. Sekiguchi, and F. Takahashi, Relic abundance of dark photon dark matter, Phys. Lett. B **801**, 135136 (2020).

[35] J. Soda and Y. Urakawa, Cosmological imprints of string axions in plateau, Eur. Phys. J. C **78**, 779 (2018).

[36] N. Kitajima, J. Soda, and Y. Urakawa, Gravitational wave forest from string axiverse, J. Cosmol. Astropart. Phys. 10 (2018) 008.

[37] P. Carenza, A. Mirizzi, and G. Sigl, Dynamical evolution of axion condensates under stimulated decays into photons, Phys. Rev. D **101**, 103016 (2020).

[38] G. Alonso-Álvarez, R. S. Gupta, J. Jaeckel, and M. Spannowsky, On the wondrous stability of ALP dark matter, J. Cosmol. Astropart. Phys. 03 (2020) 052.

[39] P. Adshead, J. T. Giblin, and Z. J. Weiner, Gravitational waves from gauge preheating, Phys. Rev. D **98**, 043525 (2018).

[40] P. Adshead, J. T. Giblin, M. Pieroni, and Z. J. Weiner, Constraining Axion Inflation with Gravitational Waves Across 29 Decades in Frequency, Phys. Rev. Lett. **124**, 171301 (2020).

[41] P. Adshead, J. T. Giblin, M. Pieroni, and Z. J. Weiner, Constraining axion inflation with gravitational waves from preheating, Phys. Rev. D **101**, 083534 (2020).

[42] See Supplemental Material at http://link.aps.org/supplemental/10.1103/PhysRevD.102.075033 for a presentation of the effects of finite dark photon mass on the GW spectrum, cosmological bounds, and GW signal templates.

[43] B. Holdom, Two U(1)'s and Epsilon charge shifts, Phys. Lett. **166B**, 196 (1986).

[44] S. Dubovsky and G. Hernández-Chifflet, Heating up the Galaxy with hidden photons, J. Cosmol. Astropart. Phys. 12 (2015) 054.

[45] This result, while perhaps surprising at first, becomes clear when we consider the limit $m_X \to 0$, where the dark photon must decouple.

[46] J. Jaeckel and A. Ringwald, The low-energy frontier of particle physics, Annu. Rev. Nucl. Part. Sci. **60**, 405 (2010).

[47] J. Jaeckel and A. Ringwald, A cavity experiment to search for hidden sector photons, Phys. Lett. B **659**, 509 (2008).

[48] S. A. Abel, J. Jaeckel, V. V. Khoze, and A. Ringwald, Illuminating the hidden sector of string theory by shining light through a magnetic field, Phys. Lett. B **666**, 66 (2008).

[49] S. A. Abel, M. D. Goodsell, J. Jaeckel, V. V. Khoze, and A. Ringwald, Kinetic mixing of the photon with hidden U(1)s

in string phenomenology, J. High Energy Phys. 07 (2008) 124.

[50] M. Ahlers, J. Jaeckel, J. Redondo, and A. Ringwald, Probing hidden sector photons through the Higgs window, Phys. Rev. D **78**, 075005 (2008).

[51] J. Redondo, Bounds on very weakly interacting sub-eV particles (WISPs) from cosmology and astrophysics, in *Proceedings, 4th Patras Workshop on Axions, WIMPs and WISPs (AXION-WIMP 2008): Hamburg, Germany* (2008), pp. 23–26, https://doi.org/10.3204/DESY-PROC-2008-02/redondo_javier.

[52] J. Redondo, Helioscope bounds on hidden sector photons, J. Cosmol. Astropart. Phys. 07 (2008) 008.

[53] A. Mirizzi, J. Redondo, and G. Sigl, Microwave background constraints on mixing of photons with hidden photons, J. Cosmol. Astropart. Phys. 03 (2009) 026.

[54] R. Essig, P. Schuster, and N. Toro, Probing dark forces and light hidden sectors at low-energy $e+e-$ colliders, Phys. Rev. D **80**, 015003 (2009).

[55] B. Batell, M. Pospelov, and A. Ritz, Exploring portals to a hidden sector through fixed targets, Phys. Rev. D **80**, 095024 (2009).

[56] A. Afanasev, O. K. Baker, K. B. Beard, G. Biallas, J. Boyce, M. Minarni, R. Ramdon, M. Shinn, and P. Slocum, New experimental limit on photon hidden-sector paraphoton mixing, Phys. Lett. B **679**, 317 (2009).

[57] J. Jaeckel and J. Redondo, Searching hidden-sector photons inside a superconducting box, Europhys. Lett. **84**, 31002 (2008).

[58] S. N. Gninenko and J. Redondo, On search for eV hidden sector photons in Super-Kamiokande and CAST experiments, Phys. Lett. B **664**, 180 (2008).

[59] M. Baryakhtar, J. Huang, and R. Lasenby, Axion and hidden photon dark matter detection with multilayer optical haloscopes, Phys. Rev. D **98**, 035006 (2018).

[60] J. E. Kim, Weak-Interaction Singlet and Strong CP Invariance, Phys. Rev. Lett. **43**, 103 (1979).

[61] M. Shifman, A. Vainshtein, and V. Zakharov, Can confinement ensure natural cp invariance of strong interactions?, Nucl. Phys. **B166**, 493 (1980).

[62] J. I. Kapusta and C. Gale, *Finite-Temperature Field Theory: Principles and Applications*, Cambridge Monographs on Mathematical Physics (Cambridge University Press, Cambridge, 2011).

[63] U. Kraemmer, A. K. Rebhan, and H. Schulz, Hot scalar electrodynamics as a toy model for hot QCD, in *From Thermal Field Theory to Neural Networks: A Day to Remember Tanguy Altherr. Proceedings, Meeting, Geneva, Switzerland, 1994* (World Scientific, Singapore, 1995), pp. 13–23, https://doi.org/10.1142/9789812830296_0002.

[64] A. Linde, Infrared problem in the thermodynamics of the yang-mills gas, Phys. Lett. **96B**, 289 (1980).

[65] D. J. Gross, R. D. Pisarski, and L. G. Yaffe, Qcd and instantons at finite temperature, Rev. Mod. Phys. **53**, 43 (1981).

[66] J. R. Espinosa, M. Quiros, and F. Zwirner, On the nature of the electroweak phase transition, Phys. Lett. B **314**, 206 (1993).

[67] This effect, which we neglect here, induces inhomogeneities in the axion field which can end the energy transfer from effects which rely on coherent resonance of gauge modes with the zero-momentum axion condensate.

[68] M. Breitbach, J. Kopp, E. Madge, T. Opferkuch, and P. Schwaller, Dark, cold, and noisy: Constraining secluded hidden sectors with gravitational waves, J. Cosmol. Astropart. Phys. 07 (2019) 007.

[69] For experiments which probe the axion-photon coupling $g_{\phi\gamma\gamma}$, we assume the KSVZ relation $g_{\phi\gamma\gamma} = -1.92\alpha_{\mathrm{EM}}/(2\pi f)$ to convert between $g_{\phi\gamma\gamma}$ and $1/f$.

[70] V. Cardoso, O. J. C. Dias, G. S. Hartnett, M. Middleton, P. Pani, and J. E. Santos, Constraining the mass of dark photons and axion-like particles through black-hole superradiance, J. Cosmol. Astropart. Phys. 03 (2018) 043.

[71] A. Arvanitaki, M. Baryakhtar, and X. Huang, Discovering the QCD axion with black holes and gravitational waves, Phys. Rev. D **91**, 084011 (2015).

[72] Additionally, we are always assuming $m_X \lesssim m/2$ and $\alpha \sim$ 10–100 such that the particle production process is efficient, see e.g., Refs. [8,29].

[73] While the exponential production of dark photons can lead to a very strong suppression [8,29], it is currently unclear whether a suppression by more than three orders of magnitude persists if backreaction effects are taken into account [28]. Otherwise, other mechanisms for depleting the axion abundance might be needed in the bottom right region of parameter space.

[74] N. Seto and A. Taruya, Measuring a Parity Violation Signature in the Early Universe via Ground-based Laser Interferometers, Phys. Rev. Lett. **99**, 121101 (2007).

[75] N. Seto and A. Taruya, Polarization analysis of gravitational-wave backgrounds from the correlation signals of ground-based interferometers: Measuring a circular-polarization mode, Phys. Rev. D **77**, 103001 (2008).

[76] T. L. Smith and R. Caldwell, Sensitivity to a frequency-dependent circular polarization in an isotropic stochastic gravitational wave background, Phys. Rev. D **95**, 044036 (2017).

[77] N. Seto, Prospects for Direct Detection of Circular Polarization of Gravitational-Wave Background, Phys. Rev. Lett. **97**, 151101 (2006).

[78] N. Seto, Quest for circular polarization of gravitational wave background and orbits of laser interferometers in space, Phys. Rev. D **75**, 061302 (2007).

[79] S. Crowder, R. Namba, V. Mandic, S. Mukohyama, and M. Peloso, Measurement of parity violation in the early universe using gravitational-wave detectors, Phys. Lett. B **726**, 66 (2013).

[80] P. Agrawal, J. Fan, M. Reece, and L.-T. Wang, Experimental targets for photon couplings of the QCD axion, J. High Energy Phys. 02 (2018) 006.